Solar Energy Materials & Solar Cells 216 (2020) 110677

Contents lists available at ScienceDirect

Solar Energy Materials and Solar Cells

journal homepage: http://www.elsevier.com/locate/solmat

Improved latent heat storage properties through mesopore enrichment of a zeolitic shape stabilizer

Cuneyt Erdinc Tas [a], Oznur Karaoglu [b], Buket Alkan Tas [a], Erdal Ertas [b], Hayriye Unal [c,**], Hakan Bildirir [b,d,*]

[a] Faculty of Engineering and Natural Sciences, Sabanci University, Istanbul, Turkey
[b] TÜBİTAK Marmara Research Centre, Food Institute, Kocaeli, Turkey
[c] Sabanci University SUNUM Nanotechnology Research Center, Istanbul, Turkey
[d] Department of Chemistry and Chemical Engineering, Chalmers University of Technology, Gothenburg, Sweden

ARTICLE INFO

Keywords:
ZSM-5
Desilication
Latent heat storage
Zeolitic shape stabilizers
Mesopore enrichment
Lauric acid
Polyethylene glycol

ABSTRACT

Latent heat storage systems are applied to keep temperature of a local environment within a constant range. The process takes place via release/storage of latent heat during freezing/melting of a corresponding phase change material embedded in a shape stabilizer, which is the scaffold keeping the phase change material stationary in its molten form. In this work, a highly siliceous ZSM-5 and modified versions thereof were chosen as shape stabilizers for molecular and polymeric phase change materials (namely lauric acid and polyethylene glycol), to be impregnated using solvent assisted vacuum impregnation. The dominantly microporous analogues, parent ZSM-5 and its acid-treated derivative, were limited to 40% uptake for each phase change material. Contrastingly, a mesopore rich analogue (as formed under basic conditions) reached 65% impregnation for lauric acid and 70% for polyethylene glycol, without any leakage at 70 °C, resulting in latent heats of 106.9 J/g and 118.6 J/g for each composite, respectively. A simple prototypical real-world application demonstrated that the prepared lauric acid and polyethylene glycol composites of mesopore enriched ZSM-5 could maintain their temperatures up to 27% and 22% lower than the ambient environment under solar heating, as well as up to 20% and 26% higher when solar heating stops. The presented findings indicate mesopore enrichment improves phase change material uptake in these low cost, non-toxic zeolitic shape stabilizers, hence making them good candidates as isolation materials to address energy loss during heating/cooling of household environments.

1. Introduction

Producing energy in a sustainable manner, without causing pollution is necessary to keep the Earth as a livable planet since conventional production processes result in significant environmental issues. Unfortunately, environmentally unfriendly energy sources are still generally preferred essentially as a consequence of costs, with significant improvements in efficiency and reductions in costs at scale required for green energy production alternatives [1–3]. Positively, a considerable volume of research has been reported with regard to addressing challenges and demonstrating improved performance of alternative energy systems, a viable solution is unlikely to be presented in the near future [4]. Therefore, reducing energy consumption is considered as a highly beneficial complementary approach, leading to a reduction in pollution resulting from excess energy use, but also a decrease the required energy-per-capita to be reached by the prospective alternative energy solution [5].

Heating is the most energy-consuming process according to International Energy Agency [6], with the use of facile techniques such as proper isolation leading to reductions in energy demand [7]. In this context, Phase Change Materials (PCMs) are interesting since their use in latent heat storage systems aims to keep the local environment within a constant temperature window [8–10]. Essentially, heat buffering process occurs via consumption of excess heat at temperatures above the melting point or the release of the stored heat at temperatures below the freezing point of the corresponding PCM. Since the latent heat of the PCM compensates for the heat change, the PCM should be selected in accordance with the aimed application. Thus, organic compounds with

* Corresponding author. TÜBİTAK Marmara Research Centre & Chalmers University of Technology, Turkey.
** Corresponding author. Sabanci University SUNUM Nanotechnology Research Center, Turkey
E-mail addresses: hunal@sabanciuniv.edu (H. Unal), hakanbildirir@gmail.com (H. Bildirir).

https://doi.org/10.1016/j.solmat.2020.110677
Received 28 February 2020; Received in revised form 15 May 2020; Accepted 21 June 2020
Available online 8 August 2020

Table 1
The long-term stability of the prepared ZSM-B composites.

PCM	T_m (°C)	ΔH_m (J/g)	%Δ H_m	T_s (°C)	Δ_s (J/g)	%Δ H_s
ZSMB/LA65 1st cycle	44.67	106.9	100	35.29	98.7	100
ZSMB/LA65 15th cycle	45.18	104.6	97.8	35.35	96.3	97.6
ZSMB/LA65 30th cycle	45.39	103.1	96.4	35.18	95.2	96.5
ZSMB/LA65 45th cycle	46.02	102.6	96.0	35.09	94.6	95.8
ZSMB/PEG70 1st cycle	59.33	118.6	100	29.17	103.9	100
ZSMB/PEG70 15th cycle	59.45	114.3	96.4	29.06	101.9	98.1
ZSMB/PEG70 30th cycle	59.16	111.6	94.1	28.71	100.5	96.7
ZSMB/PEG70 45th cycle	59.79	109.5	92.3	28.24	98.2	94.5

ΔH_m: melting enthalpy; ΔH_s: solidifying enthalpy; T_m: melting temperature; T_s: solidifying temperature % indicates the change with respect to the first cycle.

long alkyl chains such as fatty acids or polymeric materials like polyethylene glycols with different molecular weights can be utilized as useful PCMs since several of their derivatives offer different melting/-freezing points [11]. Additionally, their non-toxicity, easy processability, relatively low-costs, and inert nature also make them desirable for such use [12].

The biggest challenge in the application of PCMs is keeping the molten form stationary at elevated temperatures [13]. To solve this issue, PCMs are embedded in shape stabilizers, which are mostly porous scaffolds such as zeolites, porous carbons, metal-organic frameworks, or porous polymers [14–19]. Aside from having excellent thermal stability and conductivity, a good shape stabilizer should be able to host a large amount of PCM to have better thermal properties since the latent heat is stored by those compounds. In the literature, mesopore-rich, hierarchically porous materials are promoted as useful shape stabilizers since the mobility of long alkyl chain PCMs can be limited for microporous materials due to steric hindrance, while keeping the adsorbed PCM in the shape stabilizer (i.e. avoiding leakage) can be hard for macroporous scaffolds due to poor capillary effect [20–23].

Since their discovery in the 19th century, zeolites have been used in various fields from water softening to high-temperature catalytic cracking [24–27]. Indeed, there are examples of zeolites used in latent heat storage systems as shape stabilizers. For instance, Goitandia et al. [23] compared Zeolite Y with various inorganic shape stabilizers possessing different pore sizes. They reported the domination of the mesoporous silica over ultra-microporous zeolite Y with an impregnation of 45% for hexadecane as PCM without any leakage [23]. In another study, a frequently used zeolite, namely ZSM-5, was used as the shape stabilizer for polyethylene glycol and showed a remarkable performance with a 50% impregnation and excellent thermal conductivity [28]. In this context, introduction of mesopores among the skeleton of ZSM-5 seems interesting. Thus, in this work, we present the effect of mesopore enrichment on PCM uptake for ZSM-5 and in turn the final latent heat storage properties. Comparing the shape stabilizing performance of a pristine microporous ZSM-5 with its post-synthetically modified versions possessing altered porosity allow us to investigate specifically the effect of pore size on latent heat storage propertiesvia eliminating the effects of other variables (e.g. thermal conductivity difference) since the scaffolds have essentially the same backbone. Moreover, the choice of a molecular fatty acid (lauric acid (LA)) and a polymeric material (polyethylene glycol 4000 (PEG)) as PCMs facilitate the monitoring of structural differences such as size, shape and the number of heteroatoms on PCM loading and latent heat storage properties (see Fig. 1).

2. Experimental section

2.1. Materials

ZSM-5 type Zeolite (SiO_2/Al_2O_3 ratio of 469) was received from Acros Organics. Poly (ethylene glycol) with an average molecular weight 3500–4500 g/mol (PEG4000), lauric acid and potassium hydroxide pellets were purchased from Merck. Extra pure methanol (99.8%) was purchased from Tekkim Ltd. (Bursa/Turkey). Pure water was obtained using a Milli-Q Plus system. All chemicals were used without further purification.

2.1.1. General procedure for synthesis of ZSM-A

The preparation and characterization of ZSM-A and ZSM-B were explained in detail elsewhere [29]. The acidic treatment of ZSM-5 for the dealumination was performed in 2.5 M HCl (aq). Briefly, 50.0 g ZSM-5 was placed in a flask and 250 mL 2.5 M HCl (aq) was added. Following stirring for 6 h at 150 °C, the mixture was diluted two-fold with water. The solid was filtered and washed two times with 250 mL deionized water. Finally, the solid was dried at 120 °C overnight (under vacuum) and ZSM-A was obtained.

2.1.2. General procedure for synthesis of ZSM-B

Desilicated ZSM-5 was prepared by using nearly the same method above. 50.0 g ZSM-5 and 250 mL 2 M KOH (aq) were put in a flask, and the reaction performed 110 °C for 6 h. Subsequently, the solution was diluted with 250 mL deionized water, and the precipitate then filtered. The collected precipitate was twice washed with 250 mL water and dried at 120 °C overnight (under vacuum) to yield ZSM-B.

2.1.3. General procedure for preparation of PCM composites

Solvent assisted impregnation under vacuum was used to obtain ZSM-5, ZSM-A and ZSM-B-based PCM (LA and PEG) composites. By adjusting the total amount to 0.3 g for desired composite percentage (i.e. 0.12 g of PCM to 0.18 g shape stabilizer for 40% loading), the mixture of corresponding PCM and dried ZSM-X (in vacuum oven at 150 °C for 24 h) were added into 7.5 mL MeOH in 50 mL centrifuge tube. The charged tube was then placed in an ultrasonic water bath for 15 min and transferred to the vacuum impregnation system. Solvent removal was conducted gradually by reducing the pressure to 7–9 mbar first at room temperature by stopping the vacuum after 5 min and stirring for 5 min and repeated three times. Heating to 70 °C was then used to remove the solvent completely (in order to improve the impregnation). After solvent removal, the obtained powders were further dried in a vacuum oven for 24 h at 40 °C.

2.2. Methods

2.2.1. Instruments

Surface area measurements were performed by using the Quantachome Instrument Nova4000e (Florida, USA). Fourier Transform Infrared (FTIR) spectroscopy with an ATR system was utilized for the analysis of PCM composites. Amount of embedded PCM in composite was measured with Shimadzu Corp. DTG-60H (TGA/DTA) instrument by heating samples up to 1000 °C with a rate of 20 °C/min. Thermal properties of the PCM composites were investigated using differential scanning calorimetry (DSC; Thermal Analysis MDSC TAQ2000). Heat storage performance of PCM composites were carried out at the rate of 10 °C/min with a heating and cooling cycle between 0 and 100 °C. Stability tests were also performed using DSC from 10 to 80 °C at a rate of 20 °C/min for each cycle. All thermal measurement was carried out under nitrogen atmosphere. Thermal behavior of PCM composites under solar power light were evaluated using an Oriel LCS-100 solar simulator at 0.404 W/cm^2. Temperature changes were measured by a Hanna thermometer attached to a K-type thermocouple.

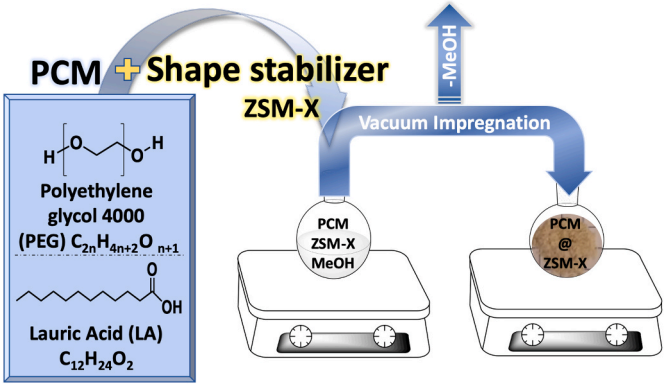

Fig. 1. Schematic representation of the composite preparation.

2.2.2. Solar simulator experiments

0.1 g of ZSMB/LA65 and ZSMB/PEG70 were placed into a 2 mL polypropylene micropipette tip and temperature change was monitored using a K-type thermocouple (as inserted into the powder).

The prepared LA and PEG containing PCM composites were irradiated in the solar simulator at 0.404 W/cm^2 power. Time-temperature curves were obtained by recording the temperatures of environment (blank), neat ZSM-B, and the corresponding composite every 2 s during heating and cooling. The measurements were repeated three times, and the calculated average values were used for time-temperature graphs.

3. Results and discussion

3.1. Comparison of shape stability of ZSM-5, ZSM-A and ZSM-B PCM composites

The properties of zeolitic structures can change significantly after simple dealumination or desilication of the framework [30]. Such modifications might lead to hierarchical porosity, which results in altered diffusion dynamics as a consequence of removal of the corresponding network unit. In this context, introducing mesopore-rich hierarchical porosity to the backbone of ZSM-5 is expected to provide favorable properties in latent heat storage systems since mesoporosity is an asset for such scaffolds in latent heat storage systems [23], and also because pristine ZSM-5 has been previously highlighted as a promising shape stabilizer for PCMs due to its good thermal conductivity, even in its microporous form [28].

Alteration to the parent ZSM-5 after acidic and basic treatments were investigated thoroughly, and explained in our previous publication [29]. Briefly, dealumination of the highly siliceous ZSM-5 (Si/Al ratio = 938) was not successful, yet the acid exposure resulted in highly microporous ZSM-A. On the other hand, base treatment of the parent material to obtain ZSM-B yielded a hierarchically porous material possessing a dominantly mesoporous character and containing less silicon. Moreover, a lower specific surface area (BET) for ZSM-B (180 m^{2}g^{-1}) was recorded in comparison to ZSM-5 (356 m^{2}g^{-1}) and ZSM-A (359 m^{2}g^{-1}) probably due to increased mesoporosity (Figs. S2 and S3).

Shape stabilizers were loaded with LA and PEG through vacuum impregnation method by mixing ZSM-X (X = 5 or A or B) and corresponding quantities of PCMs dissolved in methanol at 40–80%, (w/w) ratios, followed by ultrasonication and solvent removal under reduced pressure. Composite ZSMX/PCM powders obtained are shown in Fig. 2A.

Since impregnating shape stabilizers with the highest amount PCM

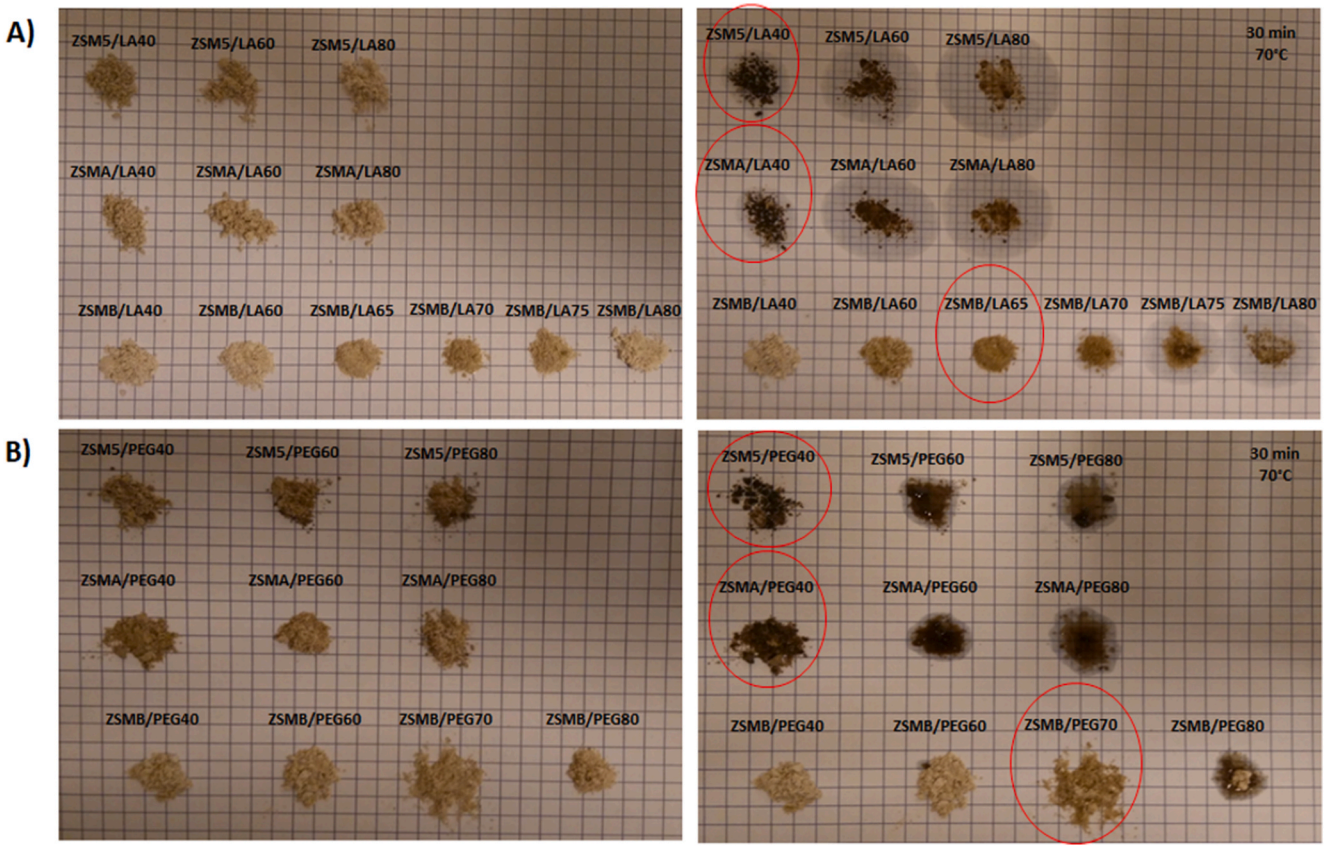

Fig. 2. The physical states of prepared ZSMX/PCM composites before (A) and after (B) heat treatment.

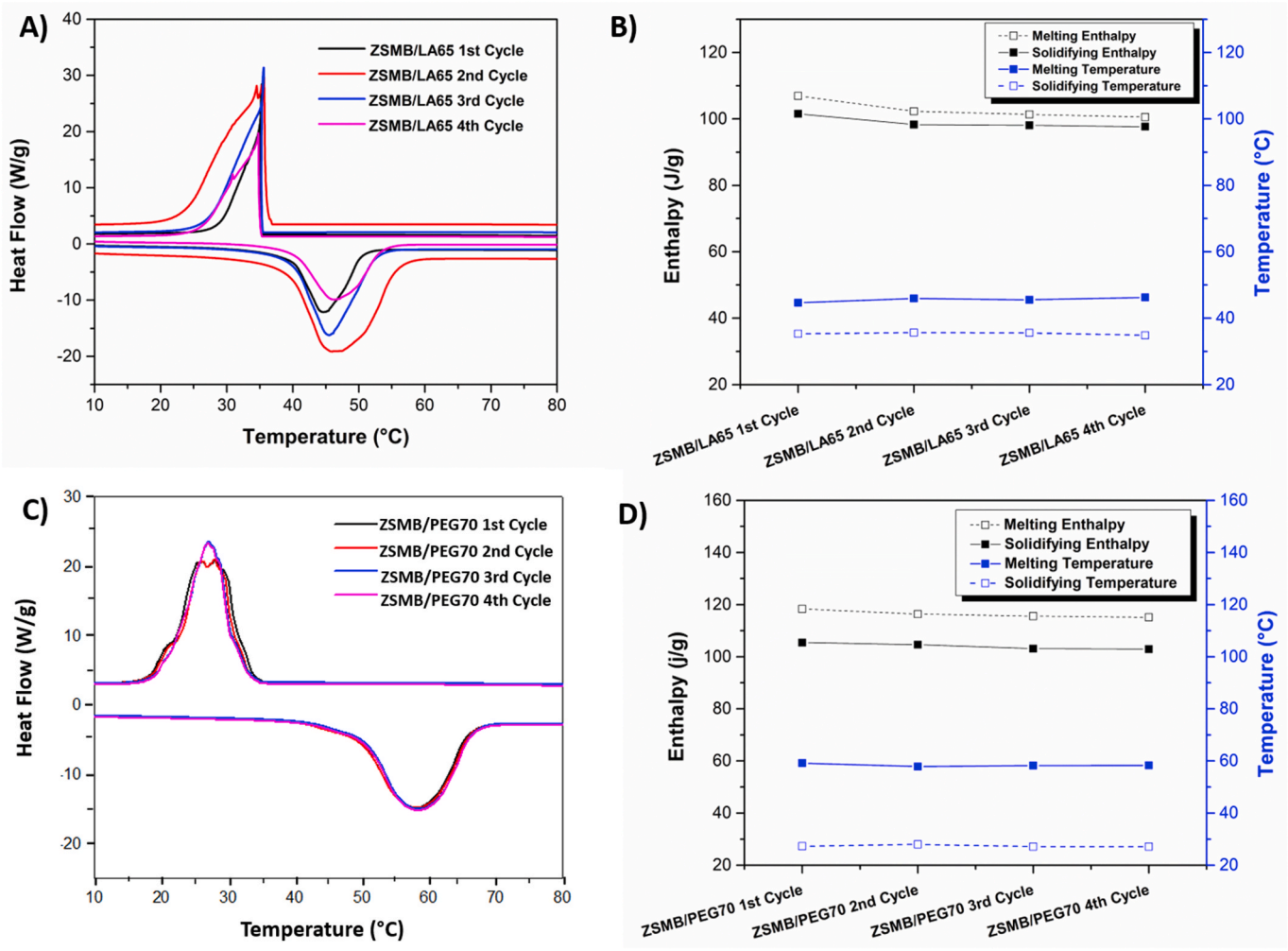

Fig. 3. DSC curves of the thermal cycle for (a) ZSMB/LA65, (c) ZSMB/LA70; (b–d) their enthalpy and transition temperature changing graphs.

without any leakage is a highly desired feature to yield optimum latent heat storage properties [31], the non-exudative maximum PCM uptake capacities of the shape stabilizers were determined via performing a leakage test at elevated temperatures. Briefly, ZSMX/PCM composites were placed on a regular paper and heated in an oven at 70 °C for 30 min, and the area below the powder was checked whether it was wet or not. As can be seen in Fig. 2B, impregnation of ZSM-A and ZSM-5 with both PCMs at ratios of 40% and above resulted in leakage, whereas the ZSM-B composites did not leak any LA and PEG even at 65% and 70% impregnation, respectively. Moreover, the actual amounts of organic PCMs loaded into ZSM-B composites were verified by thermal gravimetric analysis (TGA) under ambient atmosphere. Impregnation ratios determined by the weight losses in ZSMB/LA and ZSMB/PEG due to decomposition of organic components (for LA around 220 °C and for PEG near 410 °C) were in good agreement with theoretical values (Figure S4 and Table S1). Based on these results, the composites formed from ZSM-B were conducted for further investigations.

The exudation stability of ZSMB/LA composite at 65% impregnation (ZSMB/LA65) and ZSMB/PEG composite at 70% impregnation (ZSMB/PEG70) were evaluated by performing DSC experiments to confirm the results after the abovementioned macro-level leakage tests. Briefly, the samples were placed in a DSC sample holder and scanned for four times, during which the powders were removed from the DSC pan and put in the oven at 70 °C for 30 min after each cycle. The melting and solidifying patterns of ZSMB/LA65 and ZSMB/PEG70 were nearly the same for each cycle (Fig. 3A and C). Both melting and cooling curves of ZSMB/LA65 became slightly narrower with respect to the first cycle. This was probably due to the small amount of LA that evaporated from the composite powder at elevated temperatures during the DSC scan due to weak capillary forces [23,32]. Nevertheless, the change on the melting/solidifying enthalpies can be regarded as insignificant (Fig. 3B). On the other hand, such evaporation did not occur in case of ZSMB/PEG70 which is composed of a polymeric PCM (Fig. 3C and D).

Extended thermal stability tests of ZSMB/LA65 and ZSMB/PEG70 were employed by subjecting samples to 45 consecutive thermal cycles, during which the samples were transferred to a new pan after every 15th cycle (Table 1, Figure S5). The melting temperature of ZSMB/LA65 was detected to be only 1.5 °C lower than its initial state while its solidifying temperature remained nearly constant. On the other hand, solidifying temperature of ZSMB/PEG70 changed by only 0.9 °C while its melting temperature remained almost the same. Moreover, the melting and solidifying enthalpies also changed insignificantly, where they decreased by 4.3 J/g and 4.1 J/g, for ZSMB/LA65 and by 9.1 J/g and 5.7 J/g for ZSMB/PEG70. The negligible changes (%ΔH values; Table 1) showed that both of the prepared composites were stable after more than several melting/solidifying processes, indicating their long-term stability. Additionally, the infrared spectra of the composites before and after 45 thermal cycles also demonstrated the structural stability of the PCMs by showing nearly the same responses, particularly at ca. 2900 cm^{-1} and 900 cm^{-1} which are the vibrations of the C–H groups of the organic PCMs (Figure S6).

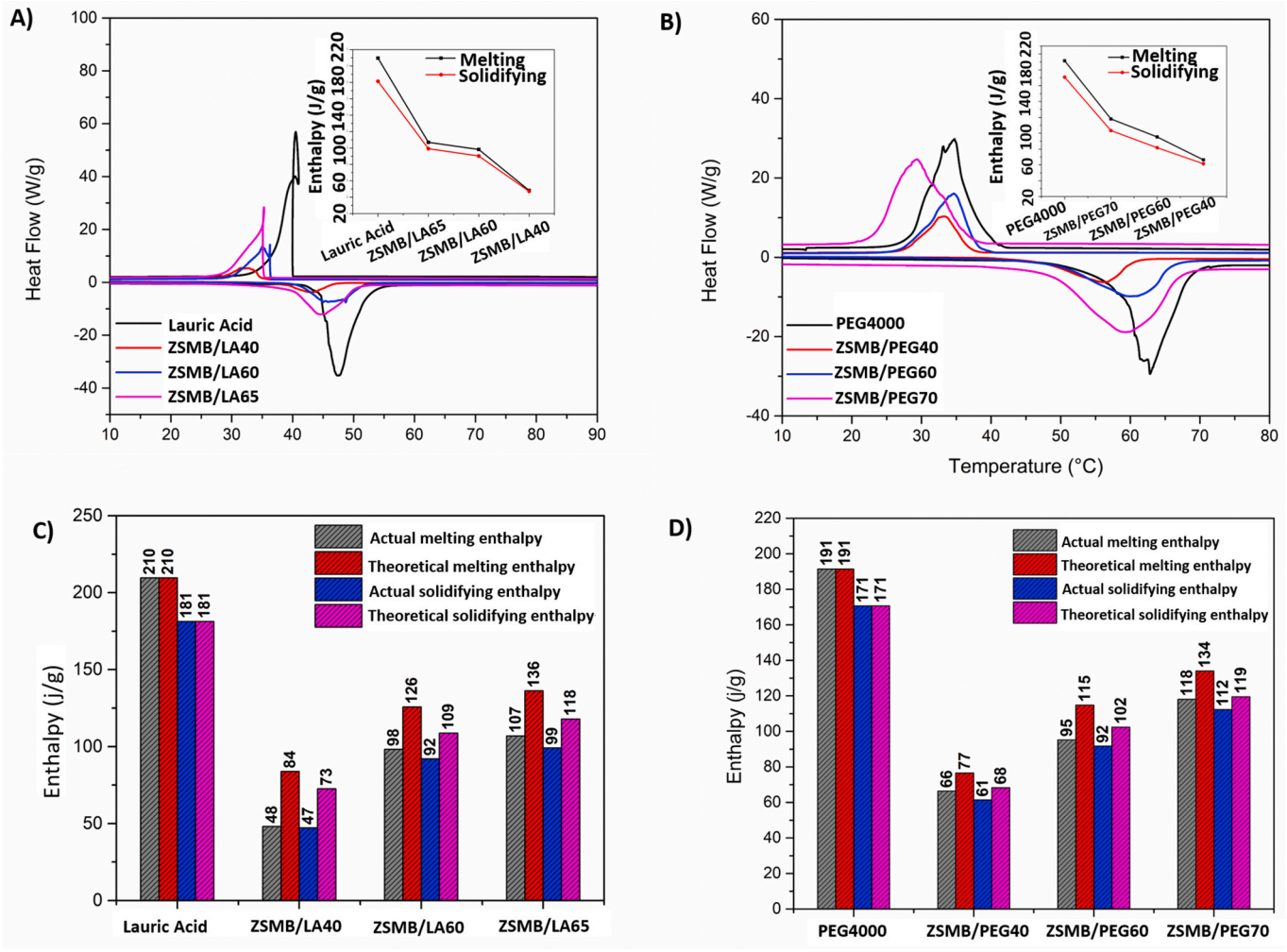

Fig. 4. DSC curves of (a) ZSMB/LA and (b) ZSMB/PEG during melting and solidifying process; enthalpies of melting and solidifying of (c) ZSMB/LA and (d) ZSMB/PEG with different PCM contents.

3.2. Thermal energy storage performance of ZSM-B based PCM composites

Latent heat storage properties of the prepared ZSM-B composites containing LA and PEG at impregnation ratios of 40% and above were investigated by DSC in order to monitor the effect of higher PCM uptake on latent heat storage properties (Fig. 4). The melting and solidifying temperatures of all composites was found to slightly shift to lower values with respect to pure LA and PEG. This was potentially caused by weak molecular interactions of PCMs with the porous shape stabilizer (e.g. capillary forces, hydrogen bonding interactions, etc.), which affect the required energies for phase transitions [33,34]. Moreover, melting and

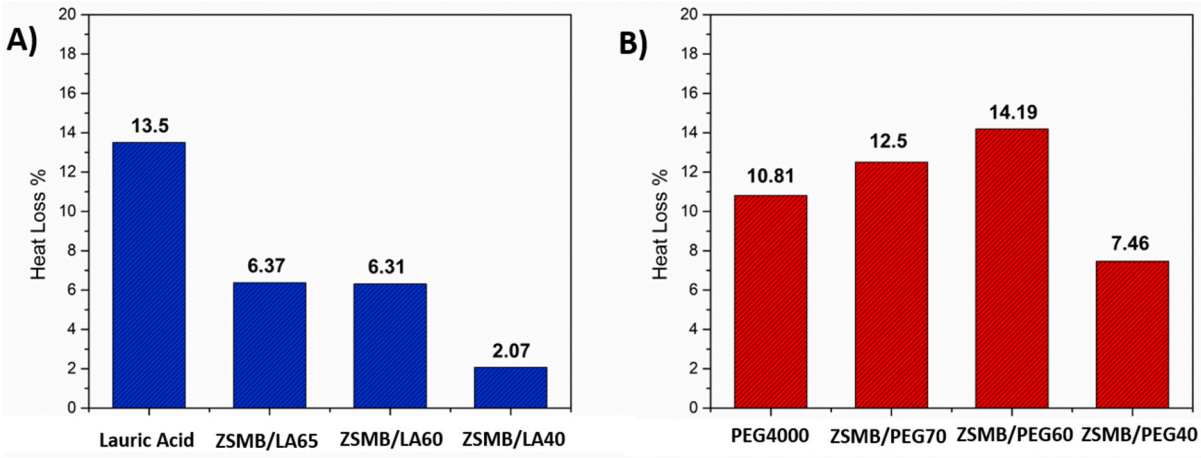

Fig. 5. Heat loss percentages of (A) ZSMB/LA and (B) ZSMB/PEG composites.

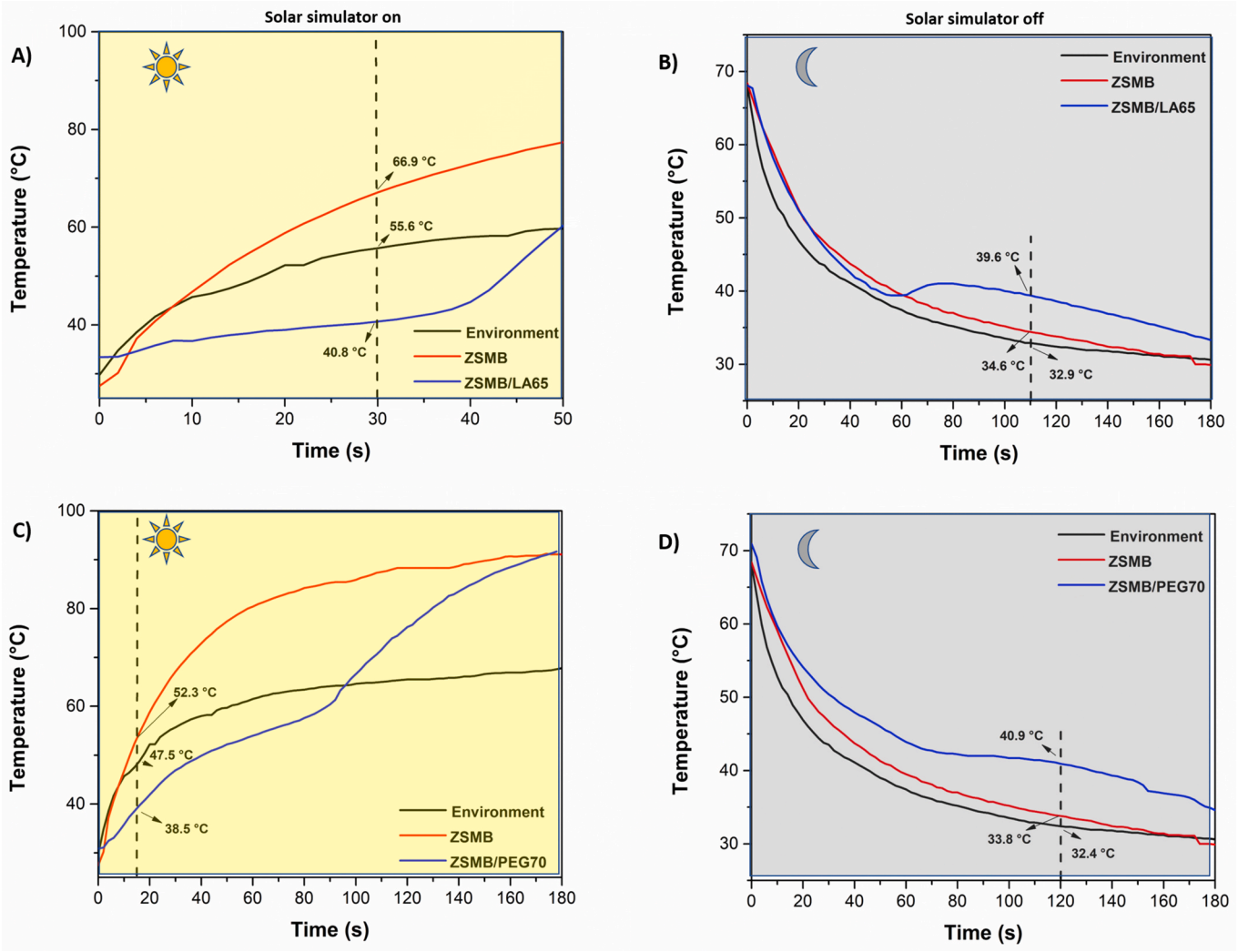

Fig. 6. Thermal behavior of (A–B) ZSMB/LA65 and (C–D) ZSMB/PEG70 composites under solar simulator irradiation.

solidifying enthalpies of the prepared composites changed proportionally with respect to their PCM impregnation ratios, confirming the successful impregnation to ZSM-B (Fig. 4C and D). The melting enthalpies of composites prepared at highest impregnation ratios, ZSMB/LA65 and ZSMB/PEG70, reached 106.9 J/g and 118.6 J/g, respectively, which are comparable enthalpies reported for similar shape stabilized PCM composites (Table S3) [28,35–41]. Especially, the composite prepared in this work via impregnation of ZSM-B with PEG presented 35.5% higher latent heat than the composite prepared with ZSM-5 [28] (also with PEG 4000) confirming the potential of ZSM-B as a high capacity PCM shape stabilizer. Notably, the actual enthalpies of all ZSM-B composites were found to be lower than the theoretical values to different extents. A significant difference was observed for ZSMB/LA40, for which the LA molecules should be hindered in the core of the scaffold as a result of the low mass fraction. Therefore, the big deviation can either be due to the possible gap between the PCM and the exterior area of the scaffold [42,43] or altered phase change behavior of the LA in such highly confined spaces [44].

Theoretical enthalpies of ZSMB/PCM composites were calculated by using Eq. (1). The actual enthalpies of pure PCMs (100% PCM content) were accepted as their theoretical enthalpies to make comparison with the ZSMB/PCM composite system.

$$\Delta H_{theo.}: (1\text{-}w)\ \Delta H_{m/s} \quad (1)$$

where "$\Delta H_{theo.}$" is theoretical latent enthalpy, "$H_{m/s}$" is the melting or solidifying enthalpy of pure PCMs, and "*w*" denotes the content of ZSM-B.

On the other hand, the variations between actual and theoretical values were less significant for the composites of PEG. Presumably, the higher heteroatom content (oxygen) of PEG or its bulkier polymeric structure (Mw: ≈ 4000 g/mol) result in strong interactions with the skeleton of zeolitic framework might reduce the strength of the capillary forces to confine the material through the core of the scaffold as deep as LA. Nevertheless, such interactions should also be limiting the (re) crystallization of the molten phase in the low loadings, hence yielding lower actual enthalpies than the theoretical [34].

The differences between melting and solidifying enthalpies (heat loss) of the prepared composites were calculated to monitor their relative latent heating and cooling performances (Fig. 5). The heat loss calculated for pure LA was considerably higher than the heat loss calculated for its composites indicating that the capillary forces of the shape stabilizer limits its evaporation [45] at elevated temperatures. Indeed, the composite with the lowest loading of LA, ZSMB/LA-40, showed nearly minimal heat loss as a consequence of the hindrance of such low amount of LA through the network. In case of the composites of the polymeric PEG, the heat loss occurs due to energy differences between melting and crystallization, which even occurs in case of the neat PEG [22,41].

3.3. Latent heat storage performances of ZSM-B based PCM composites under solar irradiation

The composites containing the highest amount of the PCMs were subjected to heating-cooling cycles by using a solar simulator as a prototype of real-world applications. Temperatures of ZSMB/LA65 and ZSMB/PEG70 composite powders were recorded under solar irradiation and also after the simulator was switched off. Even though the composites demonstrated nearly homogeneous heat buffering until their saturation points, maximum performances were highlighted in Fig. 6 (see Table S4 for more information).

The temperatures of both composites were compared to the temperature of the environment in the absence of the composites and the temperature of PCM-free ZSM-B powder as references under the same solar irradiation conditions. Accordingly, when the environment control temperature reached 55.6 °C, the temperature of ZSMB/LA65 powder was only 40.8 °C, providing 27% cooling. At this time point, the temperature of neat ZSM-B powder was 66.9 °C showing that the medium of ZSMB/LA65 composite powder was 39% cooler. Similarly, the temperature of ZSMB/PEG70 composite powder was 38.5 °C, at the time when the temperature of the environment reached 47.5 °C meaning that ZSMB/PEG70 composite powder keeps system 22% cooler than the ambient temperature.

Thermal behavior of both composites after the solar simulator was switched off was also evaluated. For ZSMB/LA65, at the time the environment temperature was 32.9 °C, the temperature of ZSMB/LA65 was 39.6 °C which corresponds to a 20% warmer medium than the environment. Similarly, ZSMB/PEG70 composite powder allowed a 26% warmer medium since its temperature was 40.9 °C while it was 32.4 °C for the blank. The results indicated that ZSMB/LA65 and ZSMB/PEG70 successfully perform latent heat storage by providing significantly cooler environments during solar heating and significantly warmer environments when the solar heating is disrupted through corresponding phase transitions.

4. Conclusions

Desilication was applied to a microporous zeolitic shape stabilizer, ZSM-5, in order to yield a mesopore rich hierarchically porous backbone in the framework to increase the amount of PCM impregnation. Even though the specific surface area dropped after the treatment, mesopore rich ZSM-B was able to hold nearly twice the amount of PCMs inside the framework with respect to other microporous analogues. The optimum non-exudative composites of ZSM-B containing 65% LA and 70% PEG were able to store latent heat up to 106.9 J/g and 118.6 J/g, respectively. Moreover, the solar simulator tests of ZSMB/LA65 and ZSMB/PEG70 indicated the latent heat storage potential of the composites via buffering the temperature change up to 27% and 22% when the solar simulator was on as well as 20% and 26% during the cooling, respectively. Our results demonstrate that the introduction of mesopore rich hierarchical porosity to microporous ZSM-5 improved the PCM impregnation capacity, hence the latent heat storage properties of the zeolitic shape stabilizer. Additionally, the solar simulator tests indicate how promising the latent heat storage systems are to keep an environment in a constant temperature to save energy spent for heating and its significant *lab-to-fab* potential via hereby presented combination of non-toxic PCMs with low-cost shape stabilizers.

Funding information

This work was partially supported by the Scientific and Technological Research Council of Turkey (TÜBİTAK) with Grant No: 215M279.

Declaration of competing interest

The authors declare that they have no known competing financial interests or personal relationships that could have appeared to influence the work reported in this paper.

Appendix A. Supplementary data

Supplementary data to this article can be found online at https://doi.org/10.1016/j.solmat.2020.110677.

References

[1] B. Liddle, P. Sadorsky, How much does increasing non-fossil fuels in electricity generation reduce carbon dioxide emissions? Appl. Energy 197 (2017) 212–221.
[2] R.B. Jackson, C. Le Quéré, R.M. Andrew, J.G. Canadell, J.I. Korsbakken, Z. Liu, G. P. Peters, B. Zheng, Global energy growth is outpacing decarbonization, Environ. Res. Lett. 13 (2018), 120401.
[3] S. Chu, A. Majumdar, Opportunities and challenges for a sustainable energy future, Nature 488 (2012) 294–303.
[4] S.J. Davis, N.S. Lewis, M. Shaner, S. Aggarwal, D. Arent, I.L. Azevedo, S.M. Benson, T. Bradley, J. Brouwer, Y.-M. Chiang, C.T.M. Clack, A. Cohen, S. Doig, J. Edmonds, P. Fennell, C.B. Field, B. Hannegan, B.-M. Hodge, M.I. Hoffert, E. Ingersoll, P. Jaramillo, K.S. Lackner, K.J. Mach, M. Mastrandrea, J. Ogden, P.F. Peterson, D. L. Sanchez, D. Sperling, J. Stagner, J.E. Trancik, C.-J. Yang, K. Caldeira, Net-zero emissions energy systems, Science 360 (2018), eaas9793.
[5] C. Amaral, R. Vicente, P.A.A.P. Marques, A. Barros-Timmons, Phase change materials and carbon nanostructures for thermal energy storage: a literature review, Renew. Sustain. Energy Rev. 79 (2017) 1212–1228.
[6] U. Collier, Renewable Heat Policies Delivering Clean Heat Solutions for the Energy Transition, Insights Series/IEC, 2018.
[7] E. Asadi, M.G. da Silva, C.H. Antunes, L. Dias, Multi-objective optimization for building retrofit strategies: a model and an application, Energy Build. 44 (2012) 81–87.
[8] M. Ahmad, A. Bontemps, H. Sallée, D. Quenard, Thermal testing and numerical simulation of a prototype cell using light wallboards coupling vacuum isolation panels and phase change material, Energy Build. 38 (2006) 673–681.
[9] A.A.A. Abuelnuor, A.A.M. Omara, K.M. Saqr, I.H.I. Elhag, Improving indoor thermal comfort by using phase change materials: A review, Int. J. Energy Res. 42 (2018) 2084–2103.
[10] Z. Rao, S. Wang, Z. Zhang, Energy saving latent heat storage and environmental friendly humidity-controlled materials for indoor climate, Renew. Sustain. Energy Rev. 16 (2012) 3136–3145.
[11] K. Pielichowska, K. Pielichowski, Phase change materials for thermal energy storage, Prog. Mater. Sci. 65 (2014) 67–123.
[12] S.S. Chandel, T. Agarwal, Review of current state of research on energy storage, toxicity, health hazards and commercialization of phase changing materials, Renew. Sustain. Energy Rev. 67 (2017) 581–596.
[13] M.M. Umair, Y. Zhang, K. Iqbal, S. Zhang, B. Tang, Novel strategies and supporting materials applied to shape-stabilize organic phase change materials for thermal energy storage–A review, Appl. Energy 235 (2019) 846–873.
[14] Y. Luan, M. Yang, Q. Ma, Y. Qi, H. Gao, Z. Wu, G. Wang, Introduction of an organic acid phase changing material into metal–organic frameworks and the study of its thermal properties, J. Mater. Chem. A 4 (2016) 7641–7649.
[15] J. Tang, M. Yang, F. Yu, X. Chen, L. Tan, G. Wang, 1-Octadecanol@hierarchical porous polymer composite as a novel shape-stability phase change material for latent heat thermal energy storage, Appl. Energy 187 (2017) 514–522.
[16] J. Li, Z. Cheng, M. Zhu, A. Thomas, Y. Liao, Facile synthesis of nitrogen-rich porous organic polymers for latent heat energy storage, ACS Appl. Energy Mater. 1 (2018) 6535–6540.
[17] J. Yang, L.-S. Tang, L. Bai, R.-Y. Bao, Z.-Y. Liu, B.-H. Xie, M.-B. Yang, W. Yang, High-performance composite phase change materials for energy conversion based on macroscopically three-dimensional structural materials, Mater. Horiz. 6 (2019) 250–273.
[18] X. Huang, X. Chen, A. Li, D. Atinafu, H. Gao, W. Dong, G. Wang, Shape-stabilized phase change materials based on porous supports for thermal energy storage applications, Chem. Eng. J. 356 (2019) 641–661.
[19] X. Zhang, Q. Lin, H. Luo, S. Luo, Three-dimensional graphitic hierarchical porous carbon/stearic acid composite as shape-stabilized phase change material for thermal energy storage, Appl. Energy 260 (2020), 114278.
[20] D. Feng, Y. Feng, L. Qiu, P. Li, Y. Zang, H. Zou, Z. Yu, X. Zhang, Review on nanoporous composite phase change materials: fabrication, characterization, enhancement and molecular simulation, Renew. Sustain. Energy Rev. 109 (2019) 578–605.
[21] H. Gao, J. Wang, X. Chen, G. Wang, X. Huang, A. Li, W. Dong, Nanoconfinement effects on thermal properties of nanoporous shape-stabilized composite PCMs: a review, Nano Energy 53 (2018) 769–797.
[22] L. Feng, W. Zhao, J. Zheng, S. Frisco, P. Song, X. Li, The shape-stabilized phase change materials composed of polyethylene glycol and various mesoporous matrices (AC, SBA-15 and MCM-41), Sol. Energy Mater. Sol. Cell. 95 (2011) 3550–3556.
[23] A.M. Goitandia, G. Beobide, E. Aranzabe, A. Aranzabe, Development of content-stable phase change composites by infiltration into inorganic porous supports, Sol. Energy Mater. Sol. Cell. 134 (2015) 318–328.
[24] A.F. Masters, T. Maschmeyer, Zeolites – from curiosity to cornerstone, Microporous Mesoporous Mater. 142 (2011) 423–438.

[25] A. Thomas, Functional Materials: From Hard to Soft Porous Frameworks, Angew. Chem. Int. Ed. 49 (2010) 8328–8344.
[26] K.V. Kumar, K. Preuss, M.-M. Titirici, F. Rodríguez-Reinoso, Nanoporous materials for the onboard storage of natural gas, Chem. Rev. 117 (2017) 1796–1825.
[27] E.T.C. Vogt, B.M. Weckhuysen, Fluid catalytic cracking: recent developments on the grand old lady of zeolite catalysis, Chem. Soc. Rev. 44 (2015) 7342–7370.
[28] C. Li, H. Yu, Y. Song, M. Zhao, Synthesis and characterization of PEG/ZSM-5 composite phase change materials for latent heat storage, Renew. Energy 121 (2018) 45–52.
[29] O. Karaoglu, G. Alpdogan, S.D. Zor, H. Bildirir, E. Ertas, Efficient solid phase extraction of α-tocopherol and β-sitosterol from sunflower oil waste by improving the mesoporosity of the zeolitic adsorbent, Food Chem. (2020), 125890.
[30] J. Pérez-Ramírez, C.H. Christensen, K. Egeblad, C.H. Christensen, J.C. Groen, Hierarchical zeolites: enhanced utilisation of microporous crystals in catalysis by advances in materials design, Chem. Soc. Rev. 37 (2008) 2530–2542.
[31] L. Miró, C. Barreneche, G. Ferrer, A. Solé, I. Martorell, L.F. Cabeza, Health hazard, cycling and thermal stability as key parameters when selecting a suitable phase change material (PCM), Thermochim. Acta 627–629 (2016) 39–47.
[32] M.-H. Yang, Y.-M. Choong, A rapid gas chromatographic method for direct determination of short-chain (C2–C12) volatile organic acids in foods, Food Chem. 75 (2001) 101–108.
[33] D. Zhang, S. Tian, D. Xiao, Experimental study on the phase change behavior of phase change material confined in pores, Sol. Energy 81 (2007) 653–660.
[34] C. Wang, L. Feng, W. Li, J. Zheng, W. Tian, X. Li, Shape-stabilized phase change materials based on polyethylene glycol/porous carbon composite: the influence of the pore structure of the carbon materials, Sol. Energy Mater. Sol. Cell. 105 (2012) 21–26.
[35] Z. Lu, B. Xu, J. Zhang, Y. Zhu, G. Sun, Z. Li, Preparation and characterization of expanded perlite/paraffin composite as form-stable phase change material, Sol. Energy 108 (2014) 460–466.
[36] Y. Konuklu, O. Ersoy, O. Gokce, Easy and industrially applicable impregnation process for preparation of diatomite-based phase change material nanocomposites for thermal energy storage, Appl. Therm. Eng. 91 (2015) 759–766.
[37] S. Song, L. Dong, Y. Zhang, S. Chen, Q. Li, Y. Guo, S. Deng, S. Si, C. Xiong, Lauric acid/intercalated kaolinite as form-stable phase change material for thermal energy storage, Energy 76 (2014) 385–389.
[38] D. Zhang, J. Zhou, K. Wu, Z. Li, Granular phase changing composites for thermal energy storage, Sol. Energy 78 (2005) 471–480.
[39] Q. Shen, J. Ouyang, Y. Zhang, H. Yang, Lauric acid/modified sepiolite composite as a form-stable phase change material for thermal energy storage, Appl. Clay Sci. 146 (2017) 14–22.
[40] T. Qian, J. Li, H. Ma, J. Yang, The preparation of a green shape-stabilized composite phase change material of polyethylene glycol/SiO2 with enhanced thermal performance based on oil shale ash via temperature-assisted sol–gel method, Sol. Energy Mater. Sol. Cell. 132 (2015) 29–39.
[41] X. Min, M. Fang, Z. Huang, Y.g. Liu, Y. Huang, R. Wen, T. Qian, X. Wu, Enhanced thermal properties of novel shape-stabilized PEG composite phase change materials with radial mesoporous silica sphere for thermal energy storage, Sci. Rep. 5 (2015) 12964.
[42] L. Xia, P. Zhang, R.Z. Wang, Preparation and thermal characterization of expanded graphite/paraffin composite phase change material, Carbon 48 (2010) 2538–2548.
[43] J. Wang, X. Jia, D.G. Atinafu, M. Wang, G. Wang, Y. Lu, Synthesis of "graphene-like" mesoporous carbons for shape-stabilized phase change materials with high loading capacity and improved latent heat, J. Mater. Chem. A 5 (2017) 24321–24328.
[44] R. Radhakrishnan, K.E. Gubbins, A. Watanabe, K. Kaneko, Freezing of simple fluids in microporous activated carbon fibers, Comp. Simul. Exp. 111 (1999) 9058–9067.
[45] R. Riesen, K. Vogel, M. Schubnell, DSC by the TGA/SDTA851e considering mass changes, J. Therm. Anal. Calorim. 64 (2001) 243–252.